

Photoelastic Design Data for Pressure Stresses in Slotted Rocket Grains

M. E. FOURNEY* AND R. R. PARMETER*
California Institute of Technology, Pasadena, Calif.

The preliminary photoelastic data of Ordahl and Williams for calculating the maximum stress in a family of slotted solid propellant rocket grains are amplified and improved in accuracy. The effect of changes in the shape of the inverse star point on the maximum stress at the star point also is investigated, and the experimental data are compared with Wilson's analytical results that used conformal mapping. Finally, an empirical formula covering the range of parameters tested is derived for possible use in integrated internal ballistics computations. The design data are useful in the elastic and viscoelastic stress analysis of free or case-bonded, internally or externally pressurized rocket grains.

THE family of grains considered in this study is similar to the one investigated by Ordahl and Williams¹ and may be characterized by four parameters: w/ρ , w/b , a'/b , as defined in Fig. 1, and N , the number of star points. Photoelastic tests have been conducted on over 80 specimens to determine the maximum elastic tangential stress for a grain subjected to a pressure loading under conditions of plane stress.

Although the tests were conducted for external pressure P_0 only, it easily may be shown² that the results may be extended to the case of arbitrary internal and external pressures. In fact, several extensions have been presented, including the case of a free grain with internal and external pressure, a case-bonded grain with both rigid and elastic case, and the effects of a linear viscoelastic material.^{2, 3}

The maximum tangential stress occurs at a position where the radial stress σ_r is known and, because of the symmetry of the slots, the shearing stress $\tau_{r\theta}$ vanishes. Thus the tangential stress may be determined directly from the isochromatic lines. These experimental data plus limit points† as $w/\rho \rightarrow 0$, with w/b constant, allow one to draw curves of σ_θ/P_0 vs w/ρ , with w/b constant, for $N = 3, 4, 5, 6$, and 8 . With the exception of the region near the limit points (w/ρ small), the N dependence of the curves is very nearly $N^{1/3}$. By plotting $N^{1/3}\sigma_\theta/P_0$, the experimental data for all values of N have been plotted in Fig. 2. If σ_θ/P_0 is required for a smaller value of w/ρ than shown on this curve, the complete curves with limit points may be found in Ref. 2.

The effect of changes in the inverse star point (point A of Fig. 1) on the value of σ_θ/P_0 was determined. An investigation of the dependence of σ_θ/P_0 on a'/a was made and found to be negligible for $a'/a < 0.6$.

Wilson⁴ has found an analytical solution for a four-star configuration similar to some of those tested. A comparison of the experimental data and Wilson's theoretical solution is presented in Fig. 3. This excellent agreement, plus the large number of mutually consistent test points, lends considerable strength to the curves presented. They will be found to differ by as much as 50% from the data presented by Williams and Ordahl.

Presented at the ARS Launch Vehicles: Structures and Materials Conference, Phoenix, Ariz., April 3-5, 1962; revision received January 2, 1963. The authors wish to acknowledge the support of the Propulsion Development Department, U. S. Naval Ordnance Test Station, China Lake, Calif., during this investigation.

* Graduate Students, Graduate Aeronautical Laboratories; also Consultants, Mathematical Sciences Corporation, Altadena, Calif.

† The limit points presented in Ref. 1 are in error.

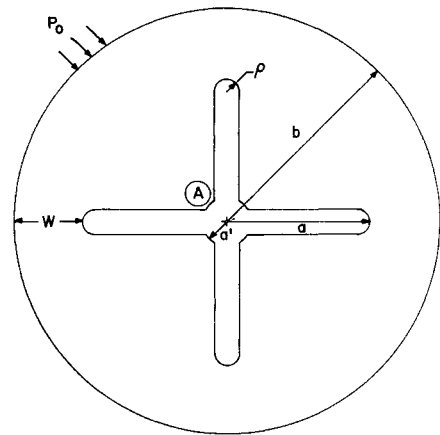


Fig. 1 Geometry

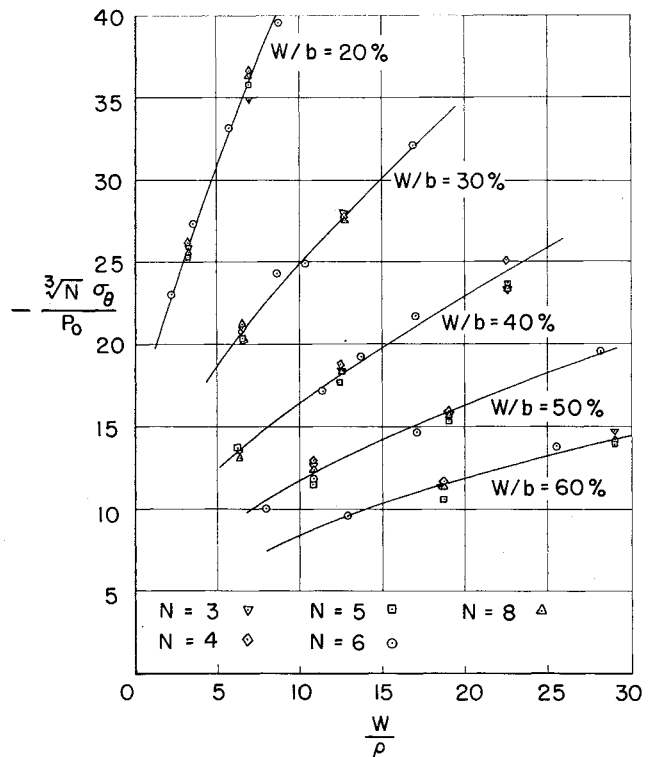


Fig. 2 Tangential stress at star point

An empirical formula has been derived, for possible use in machine computations of the stress history during a ballistic mission, which fits the experimental curves within 5% over most of the range of interest and within 10% overall. This relation is

$$\frac{\sigma_\theta}{P_0} = - \left[1 + \left\{ \left(\frac{6}{N} \right)^{1/3} - 1 \right\} \cdot \left\{ 1 - \exp \left[-0.4 \times \left(\frac{W}{\rho} - \frac{w/b}{1 - w/b} \right) \frac{b}{w} \right] \right\} \cdot \left[\left\{ 0.52 \left(\frac{w}{b} \right)^{-1.77} - 0.80 \right\} \left(\frac{w}{\rho} \right)^{[1.90 (w/b)^{0.175} - 1.0]} + 1.7 \left\{ 1 - 15.8 \exp \left[-18.4 \left(\frac{w}{b} \right) \right] \right\} \right] \right] \quad (1)$$

A group at New York University⁵ has correlated the data of Fig. 2 with the results from internally notched strips under axial tension. Using Eq. 1, σ_θ/P_0 was calculated for $N = 2$

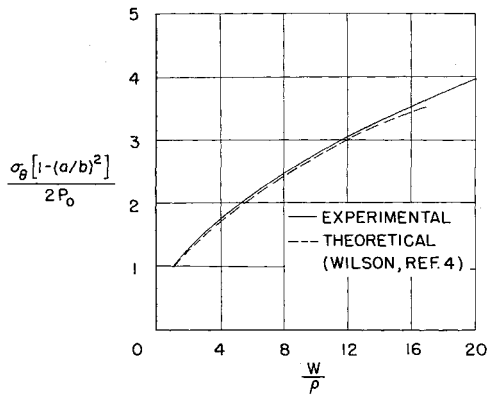


Fig. 3 Comparison of theory and experiment for $N = 4$

and compared to a notched strip. The following relation was deduced:

$$\frac{\sigma_\theta}{P_0} = - \left(\frac{2 - w/b}{w/b} \right)^{1/2} N^{-1/3} \times \left[1 + 2 \left\{ \frac{W}{\rho} \left(\frac{1 - w/b}{w/b} \right) \right\}^{1/2} \right] \quad (2)$$

This expression fits the data quite well except in the region near the limit points as $w/\rho \rightarrow 0$.

In summary, the results of these tests indicate that the maximum tangential stress at the star point can be reduced in the following ways: 1) increasing the fillet radius, 2) increasing the web fraction, and 3) increasing the number of star points. It also has been shown that major geometrical changes in the inverse star-point region have little effect on the maximum stress. However, one should not conclude that the maximum stress is unaffected by small geometrical changes in the star-point region. Recent tests have shown that relatively minor changes in the star-point contour can reduce the maximum stress by more than a factor of 3.

References

- ¹ Ordahl, D. D. and Williams, M. L., "Preliminary photoelastic design data for stresses in rocket grains," Jet Propulsion 27, 657-662 (1957).
- ² Fourney, M. E. and Parmeter, R. R., "Stress-concentrations for internally perforated star grains," Bur. Naval Weapons, NAVWEPS Rept. 7758 (December 1961).
- ³ Williams, M. L., Blatz, P. J., and Schapery, R. A., "Fundamental studies relating to systems analysis of solid propellants," GALCIT SM 61-5, Calif. Inst. Tech. (February 1961).
- ⁴ Wilson, H. B., Jr., "Stresses owing to internal pressure in solid propellant rocket grains," ARS J. 31, 309-317 (1961).
- ⁵ Becker, H., private communication, New York Univ. (1962).

A Simple MHD Flow with Hall Effect

RICHARD H. LEVY*

Avco-Everett Research Laboratory, Everett, Mass.

IN magnetohydrodynamics, the Hall effect rotates the current vector away from the direction of the electric field and generally reduces the level of the force that the magnetic field exerts on the flow. It usually is measured by the param-

Received by IAS November 19, 1962. This research was supported by Headquarters, Ballistic Systems Division, Air Force Systems Command, U. S. Air Force Contract No. AF 04(694)-33.

* Principal Research Scientist.

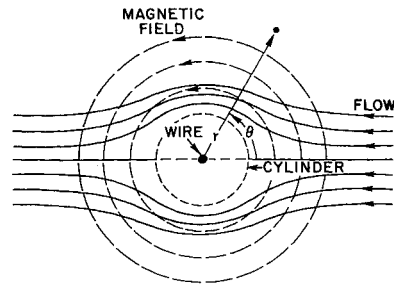


Fig. 1 Illustration of problem studied. The flow past the cylinder is unperturbed, and the current pattern is to be determined

ter $\omega\tau$, where $\omega = eB/m$ is the angular velocity of the electron orbits around the field lines, and τ is the mean time between scattering collisions for the electrons. The form of Ohm's law which accounts for the Hall effect is¹

$$\mathbf{j} = \sigma(\mathbf{E} + \mathbf{v} \times \mathbf{B}) - (e\tau/m)\mathbf{j} \times \mathbf{B} \quad (1)$$

This note will describe a simple flow in which the Hall currents can be calculated exactly and the results compared with those that follow from the usual simplifying assumptions of reducing in fixed ratios the conductivities parallel and perpendicular to the field lines.

Consider a flow of the type illustrated in Fig. 1. A wire carrying current I coincides with the z axis, and the magnetic Reynolds number is assumed small so that (in cylindrical coordinates)

$$\mathbf{B} = (0, \mu_0 I / 2\pi r, 0) \quad (2)$$

The flow is assumed to be given, and the velocity vector is restricted to be of the form

$$\mathbf{v} = U \{ [-1 + (a^2/r^2)] \cos\theta, [1 + (a^2/r^2)] \sin\theta, 0 \} \quad (3)$$

which represents uniform two-dimensional flow without circulation past a cylinder of radius a , with velocity U at infinity. In the absence of the Hall effect, the current is in the z direction and is given by

$$\begin{aligned} j_z &= (-\sigma U \mu_0 I / 2\pi r) [1 - (a^2/r^2)] \cos\theta \\ &= -(N_e e U) (\omega\tau) [1 - (a^2/r^2)] \cos\theta \end{aligned} \quad (4)$$

where $\sigma = N_e e^2 \tau / m$, N_e being the electron density. However, the Hall effect will reduce this current and also produce a current pattern in the plane of the flow. A nondimensional distance is defined by

$$\bar{r} = (\omega\tau)^{-1} = 2\pi m r / \mu_0 e \tau I \quad (5)$$

and let $r = a$ correspond to $\bar{r} = \bar{a}$. Since the current vector

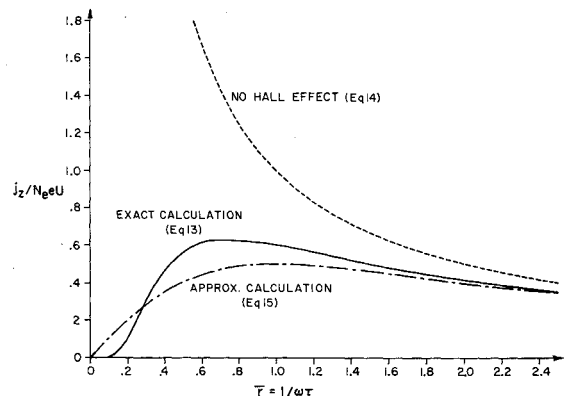


Fig. 2 Illustration of the reduction in the conduction current due to the Hall effect as calculated exactly and approximately